



Research Article

Subhasish Sarkar*, Arghya Mukherjee, Rishav Kumar Baranwal, Jhumpa De, Chanchal Biswas, and Gautam Majumdar

Prediction and parametric optimization of surface roughness of electroless Ni-Co-P coating using Box-Behnken design

<https://doi.org/10.1515/jmbm-2019-0017>

Received Oct 25, 2019; accepted Nov 24, 2019

Abstract: The current study focuses on the parametric optimization of electroless Ni-Co-P coating considering surface roughness as a response using Box-Behnken Design (BBD) of experiment. The two bath parameters namely the concentration of cobalt sulphate and sodium hypophosphite were varied along with the bath temperature to predict the variation in surface roughness. Analysis of variance (ANOVA) method has been applied to determine the interactions of the substantial factors which dominate the surface roughness of the coating. The process parameters for surface roughness of the coating were optimized by successfully utilizing the statistical model of Box-Behnken Design (BBD) of experiment. From the BBD model, the optimum condition for the deposition of the coating has been evaluated. In that specific condition, the surface roughness of the as-deposited coating is found to be $0.913\mu\text{m}$. Scanning Electron Microscopy (SEM), Energy Dispersive X-ray Spectroscopy (EDX), and X-Ray Diffraction (XRD) study have been utilized to characterize the electroless Ni-Co-P coating deposited in optimized condition.

Keywords: Electroless coating, Box-Behnken design, surface roughness, ANOVA, SEM, EDX, XRD analysis

1 Introduction

During the past two decades, electroless coating has proved to be an innovative technique of surface coating methodology. It was Brenner and Riddell who were the first ones to develop electroless coating in 1946 [1]. It is basically a process that involves the deposition of nickel in several combinations of alloys and composites [2], each having its exclusive set of properties, from an aqueous solution onto the surface of a substrate, without the applying electricity. Unlike the conventional electroplating process [3], which involves direct current for the reduction of Nickel ions in the electrolyte; this is a chemical technique where the Nickel ions are reduced with the help of a reducing agent and deposited onto the catalytically activated substrate [4]. Along with a great quality of the deposit, electroless coatings have great hardness [5], anti-corrosion [6], wear and abrasion resistance [7, 8] properties, which is the sole reason for its wide application in the field of aerospace [9], automobile [10], mining [11], marine, biomedical industries [12, 13], etc.

Since its first development, the electroless coating has been a topic of research and has gone through various modifications and developments [14]. The development of poly-alloy coatings [15] is one such important development, which allows us to add different elements/complexes to the binary electroless coatings like Ni-P or Ni-B [16, 17] and hence alter their physical or chemical properties effectively [18, 19]. The additional element to be added to the binary electroless coatings was chosen depending upon the requirement of physical or chemical properties required to be imparted to the coating for improving the pre-existing properties [20]. Cobalt is best suited for imparting electromagnetic properties and improving the thermal stability of the electroless coatings [21]. Cobalt being a ferromagnetic material [22], reduces the residual magnetism and improves the coercive force of the electroless Ni-Co-P deposits [23]. Correspondingly, copper, used frequently in our day-to-day lives, is a

*Corresponding Author: Subhasish Sarkar: Department of Mechanical Engineering, Jadavpur University, Kolkata-700032, India; Email: subha.jumechanical@gmail.com

Arghya Mukherjee, Rishav Kumar Baranwal, Gautam Majumdar: Department of Mechanical Engineering, Jadavpur University, Kolkata-700032, India

Jhumpa De: Department of Mechanical Engineering, Academy of Technology, Hooghly-712121, India

Chanchal Biswas: Department of Metallurgical and Materials Engineering, Jadavpur University, Kolkata-700032, India



soft, malleable and ductile material with a very high electrical and thermal conductivity [24]. Hence, electroless Ni-Co-P coated copper substrates have lightweight, great magnetic shielding effects, corrosion resistance, and thus can be used in high-density disks [25].

Ni-P/Ni-B electroless coatings have found great applications in industries where good hardness and anti-corrosion rates are required [26]. Cobalt's introduction into the binary coating has improved surface properties in the past [27, 28]. Hence, Ni-Co-P coating has been electrolessly deposited in order to improve the surface roughness of the copper substrate. A fine layer of thickness $2\mu\text{m}$ has been deposited during the process. The reason behind such a thin layer of deposition is that once the metal is being deposited, the activated surface is no longer in contact with the electroless bath [29]. The deposited metal is in contact with the bath, which does not allow a further reaction to take place. Hence, at such a low thickness of deposition, it is very important to maintain the surface roughness at the minimum value since this property of the coating is co-related to other properties like friction and wear [30], which reduce the life of the coatings by exposing the substrate to increased corrosion and wear [31, 32], thereby increasing the cost.

This research aims at optimizing the surface roughness to the minimum, by varying different bath parameters at different levels using the Box-Behnken mathematical modeling tool [33] and determining the significant parameters along with their interactions. An effort has been made to generate the model values and comparing it with the experimental ones. It was witnessed that the coatings' experimental and modeling responses were identical. Hence, this modeling predicted the accurate surface roughness without experimentally performing it.

2 Experimental methodology

2.1 Synthesis of the coating

The copper substrate was cut from copper foil (99.0% pure, LobaChemie), which was present in the rolled form. Electroless Ni-Co-P coating was deposited over copper substrates of size $20 \times 15 \times 0.1 \text{ mm}^3$ in our current study. The substrates were first cleaned with distilled water. Acid pickling was done to the surface of the substrates followed by cleaning with distilled water again. Subsequently, palladium chloride (PdCl_2) solution, pre-heated to 55°C , was used to activate the surface of the substrates. The bath parameters were pre-determined by trial and error methods.

Once the surface activation is done, the substrates were dipped in the electroless bath. The deposition of the coatings was carried out in different concentrations & temperatures along with fixed time, bath volume and pH value. The composition of the bath is given in Table 1.

Table 1: Bath composition

Bath composition	Quantity
Nickel sulphate ($\text{NiSO}_4 \cdot 6\text{H}_2\text{O}$)	25g/L
Cobalt sulphate ($\text{CoSO}_4 \cdot 7\text{H}_2\text{O}$)	10/15/20g/l
Sodium hypophosphite ($\text{NaH}_2\text{PO}_2 \cdot \text{H}_2\text{O}$)	20/25/30g/l
Tri-sodium citrate dihydrate ($\text{Na}_3\text{C}_6\text{H}_5\text{O}_7 \cdot 2\text{H}_2\text{O}$)	15g/L
Ammonium sulphate ($(\text{NH}_4)_2\text{SO}_4$)	10g/L
pH value	5
Time	1hr
Bath volume	250cm^3
Temperature	$80^\circ\text{C}/85^\circ\text{C}/90^\circ\text{C}$

To ensure uniform deposition of the coating, the samples were kept immersed in the bath for 1 hour. Then, the as-deposited substrates were taken out of the bath and thoroughly rinsed in distilled water. Then the sample is mounted with the aid of epoxy resin for holding appropriately. Finally, the substrate was ready for the test.

2.2 The design factor for evaluating the surface roughness of the coating

The response of the coatings was measured calibrating with the Talysurf with the standard specimen; then fixing the same setup, 17 coated copper samples were measured. 17 runs were considered to synthesize the coating following the Box-Behnken Design of experiments. After taking 3 runs of the same sample, their average was taken for final evaluation. The instrument was re-checked with the standard specimen.

2.3 Evaluation of surface roughness

The surface roughness (Ra) value of the substrate was measured using a micrometer. The surface roughness of the mounted samples was calculated by Talysurf machine

Table 2: Variables of Box-Behnken Design

Variables	Unit	Significant	Values				
			Lower	Higher			
Concentration of cobalt sulphate	gm/cc	A	10	20	10	15	20
Concentration of sodium hypophosphite	gm/cc	B	20	30	20	25	30
Temperatures	Degree	C	80	90	80	85	90

by Taylor Hobson Precision Instrument Surtronic 3+. Taly-surf is an instrument used for measuring the surface texture. This method is based on a stylus traversing the surface. The stylus of the instrument generates magnifications of the signals, which are done electrically. The magnitude of the current can be varied as it depends upon the impedance of the coil. It varies as the air gap between the pole and the coil is varied. Surface roughness was measured using a contact method. The instrument has a diamond stylus with a tip radius of 4.9 μm . The surface profile obtained by the stylus is displayed on the LCD screen of the instrument. The Talyprofile software was used for the estimation of the surface roughness parameter.

2.4 Optimization of process parameters of coating considering surface roughness as a response using Box-Behnken design

The three parameters are: (i) concentration of cobalt sulphate (A), (ii) concentration of sodium hypophosphite (B), (iii) temperatures (C) each of which is evaluated at three coded levels viz. lower (-1), middle (0), higher (+1), as shown in Table 2.

Design of experiment is a mathematical tool, which saves time and has proved to be cost-effective by lowering the number of experimental runs to compute the optimum coating parameters such that the coating is formed with optimum surface roughness. The surface roughness of the electroless coating (in this case Ni-Co-P coating) depends on many factors like the concentration of nickel sulphate, sodium hypophosphite and cobalt sulphate used in the electroless bath, the temperature at which the samples are prepared, the concentration of bath stabilizers used, pH of the bath, etc. Out of these, in this experiment, we have chosen Concentration of cobalt sulphate, concentration of sodium hypophosphite (reducing agent), and temperature of the bath as the varying factors on which the surface roughness of the coating depends. To get the optimized values of the varying factors, we have used Box-Behnken Design (BBD) of experiment. The Box-Behnken

design is a response surface methodology (RSM) design that necessitates three levels in order to run an experiment. 17 set runs are performed by the model as shown in Table 3.

Design expert 9 software was utilized to carry out the 17 set runs and it followed a second-order quadratic equation (equation no-1) in order to calculate the surface roughness of the coated samples. The final equations are mentioned as follows:

Final equation in terms of coated factors:

$$\begin{aligned} \text{Surface roughness} = & +0.91 + (0.045 * A) & (1) \\ & + (0.062 * B) + (2.75 * E) - (.003 * C) - (0.074 * A * C) \\ & - (0.049 * B * C) - (0.23 * A^2) - (0.068 * B^2) \\ & + (0.33 * C^2) \end{aligned}$$

Final equation in terms of actual factors:

$$\begin{aligned} \text{Surface roughness} = & +6.79645 & (2) \\ & - (0.028740 \times \text{cobalt sulphate}) \\ & + (0.3590 \times \text{sodium hypophosphite}) \\ & - (0.24491 \times \text{temperature}) - (2.96000E) \\ & - (0.003 \times \text{cobalt sulphate} \times \text{sodium hypophosphite}) \\ & + (4.58000E) - (0.003 \times \text{cobalt sulphate} \\ & \times \text{temperature}) - (1.96000E) - (0.003 \\ & \times \text{sodium hypophosphite} \times \text{temperature}) - 9.25200E \\ & - (0.003 \times \text{cobalt sulphate}^2) - 2.7100E - (0.003 \\ & \times \text{sodium hypophosphite}^2) + 1.32800E - (0.003 \\ & \times \text{temperature}^2) \end{aligned}$$

p-value along with the significance of the individual coefficients was evaluated with the aid of the above equations. Smaller *p*-values indicate higher significance of the corresponding factors. The independent variables A, B, C, the interacting variables AB, AC, BC, the quadratic variables A^2 , B^2 , C^2 were all significant in nature.

Table 3: The set of experimental variables of the Box-Behnken design (BBD) for evaluating surface roughness

Number of runs	Actual value			Coded value			Surface roughness (Ra)
	Cobalt sulphate	Sodium hypophosphite	Temperature	Cobalt sulphate	Sodium hypophosphite	Temperature	
	X1	X2	X3	Z1	Z2	Z3	
1	15	30	90	0	+1	+1	0.817
2	10	25	90	-1	0	+1	0.582
3	15	20	90	0	-1	+1	0.853
4	10	20	85	-1	-1	0	0.402
5	15	25	85	-1	0	0	0.919
6	20	25	80	+1	0	-1	0.604
7	20	20	85	+1	-1	0	0.625
8	15	20	80	0	-1	-1	0.827
9	20	25	90	+1	0	+1	0.916
10	15	25	85	0	0	0	0.913
11	20	30	85	+1	+1	0	0.663
12	15	25	85	0	0	0	0.908
13	15	25	85	0	0	0	0.91
14	10	25	80	-1	0	-1	0.728
15	10	30	85	-1	+1	0	0.736
16	15	25	85	0	0	0	0.878
17	15	30	80	0	+1	-1	0.987

3 Results and discussion

Process optimization is defined as the discipline of coordinating a process in order to optimize a specified set of parameters without defying the constraints of the process. The objective is to maximize one or more process parameters while maintaining all others within their limits during the optimization of a process. In the present study, Box-Behnken experimental design (BBD) is used to deliver the required information for modeling with various independent variables in order to determine the optimized condition. The influence of process parameters on the response factor is quite necessary to perceive. Basically, it requires a set of experiments whose number is directly proportional to the number of process parameters. BBD is a very advantageous tool for minimizing the total number of experiments without the loss of generality because of the fact that it can deliver the minimum number of experiments along with a second-order polynomial model as a function of the independent process parameters.

3.1 Analysis of variance (ANOVA)

ANOVA is a robust mathematical structure for determining the substantial parameters taking place in a process.

F-value is the ratio of the summation of the square of the factors to the variance of the errors which aids in finding the significant factors. Hence a higher value of F will recommend a comparatively better factor with respect to others. ANOVA is not an optimization tool but a tool through which we can determine the factors which are significant in the evaluation of the surface roughness of the coating. The interactions between the different levels of different factors also play a significant role in the response of the coatings. The ANOVA analysis works on the F-ratio and the *p-value*. However, a more accurate evaluation is done using *p-value*. If the *p-value* exceeds the value of 0.05, then the factors/interactions are deemed to be insignificant. ANOVA results of the response surface quadratic models for surface roughness of the coating are presented in Table 4, which shows the Model F-value of 14.12 inferring that the model is significant.

The percentage of occurrence of such high F-value due to noise was only 0.01. The value of Model Prob>F less than 0.05 specified that the model terms were substantial. In this case, A, B, C, AB, BC, A², B², C² were the substantial model terms. As per the table, R-Squared of 0.9478 was in a sensible agreement with the Adj R-Squared of 0.8807 due to the fact that their difference was less than 0.2. Adeq Precision measured the signal to noise ratio and a value greater than 4 was suitable. This work exhibited a ratio of

Table 4: Results of the model

Statistical results of the ANOVA	
Model F-value	14.12
Model Prob>F	< 0.05
C.V.%	7.05
R-Squared	0.9478
Adj R-Squared	0.8807
Pred R-Squared	0.2011
Adeq Precision	13.128

13.128 signifying adequate signal. This model can be used to circumnavigate the design space. The coefficient of variance (C.V) % for surface roughness was calculated to be 7.05%. In view of the values of all the parameters of the ANOVA results, the model was thus found to be significant in this study.

3.2 The analysis of the 3D response surface plots along with the contour plots

The interactions amongst the factors can be illustrated from Figures 1-3. The absence of an intersection between the plots states that no noteworthy interaction has taken place. However a steeper graph with intersection points recommends substantial interactions between the factors. Figure 1 displays the second-order 3D response surface plot along with the contour plot of surface roughness as a function of the concentration of cobalt sulphate and concentration of sodium hypophosphite.

Figure 2 displays surface roughness along with the contour plot as a function of the concentration of Cobalt Sulphate and temperature. Figure 3 displays surface roughness along with the contour plot as a function of the concentration of Sodium Hypophosphite and temperature.

The response surface plot in Figure 1A specifies that the surface roughness increases with an increase in the concentration of cobalt sulphate and concentration of sodium hypophosphite. Figure 2A depicts that the surface roughness increases with the concentration of cobalt sulphate and the maximum is achieved at a bath temperature of 85°C. Figure 3A shows that the surface roughness increases with the concentration of sodium hypophosphite and the maximum is achieved at 85°C bath temperature. By relating the contour plots in Figure 1B, 2B and 3B, it can be implied that the concentration of cobalt sulphate and sodium hypophosphite have more influence on the surface roughness than temperature.

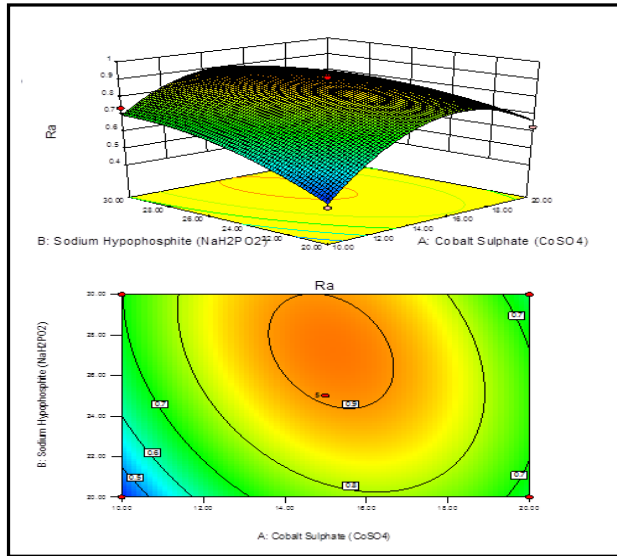


Figure 1: The second-order 3D response surface plot along with a contour plot showing the interaction effect of X1 and X2 with response to Ra

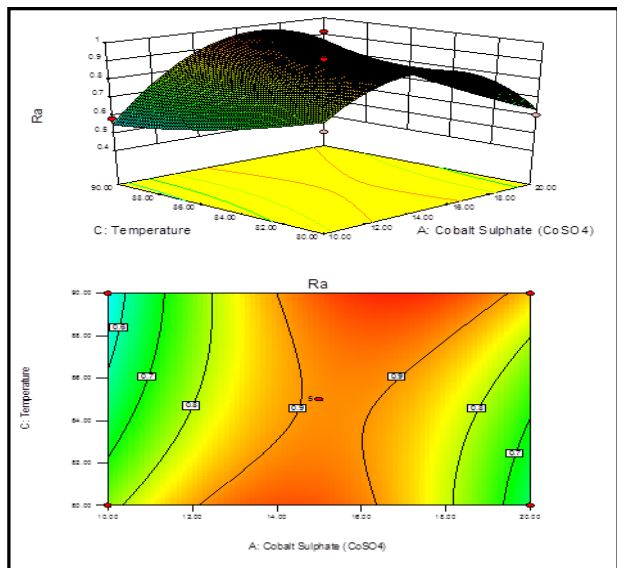


Figure 2: The second-order 3D response surface plot along with a contour plot showing the interaction effect of X1 and X3 with response to Ra

From the analysis of Figures 1-3, the optimization results of the model for surface roughness of the coated substrates are evaluated and consequently, the optimized data of concentration of cobalt sulphate and concentration of sodium hypophosphite are found out to be 15 g/L and 25 g/L, respectively along with a bath temperature of 85°C. The interaction plot of ANOVA suggests that the interactions, cobalt sulphate-temperature, sodium hypophosphite-temperature, and cobalt sulphate-

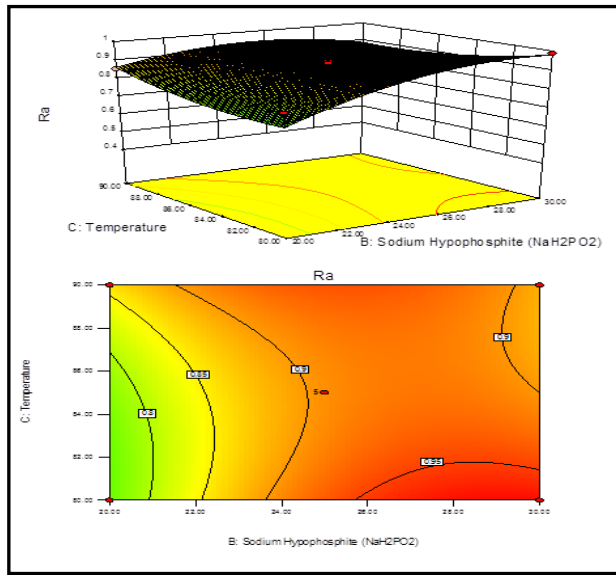


Figure 3: The second-order 3D response surface plot along with a contour plot showing the interaction effect of X2 and X3 with response to Ra

sodium hypophosphite are quite substantial in the determination of the surface roughness of the optimized coating.

3.3 Comparison of the experimental and model value analysis

Bestowing upon the model, the 17 sets of experiments have provided us with the experimental and model values of surface roughness. Table 5 contains the recorded experimental and model values where the latter were determined using Eq. 2.

The deviation of the experimental results from values given by the model is found to be less than 1%. Thus, from the results, it can be inferred that the experimental values match the model substantially. Graphical analysis of the experimental and model values with a set of experiments is given in Figure 4.

3.4 Characterization of the substrates

3.4.1 Optical microscopy and Scanning Electron Microscopy of the copper substrate

Figures 5a and 5b show the Optical Microscopy Image of the copper substrate with ferric chloride etching and SEM of the copper substrate without etching. Elongated lamel-

Table 5: Comparison of the experimental and model values

Set of expt.	Experimental value	Model value	Error in %
1	0.817	0.88675	-0.0007
2	0.582	0.55075	0.00031
3	0.853	0.86075	-0.00008
4	0.402	0.4255	-0.00024
5	0.919	0.9056	0.00013
6	0.604	0.63525	-0.00031
7	0.625	0.6635	-0.00039
8	0.827	0.75725	0.0007
9	0.916	0.86975	0.00046
10	0.913	0.9056	0.00007
11	0.663	0.6395	0.00024
12	0.908	0.9056	0.00002
13	0.91	0.9056	0.00004
14	0.728	0.77425	-0.00046
15	0.736	0.6975	0.00039
16	0.878	0.9056	-0.00028
17	0.987	0.97925	0.00008

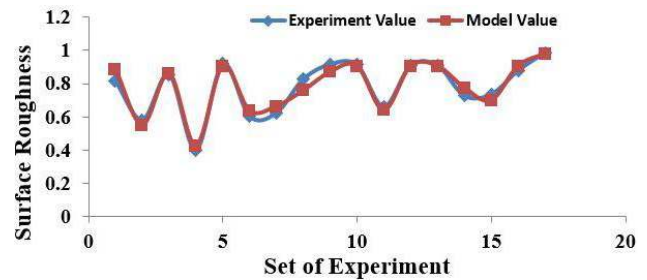
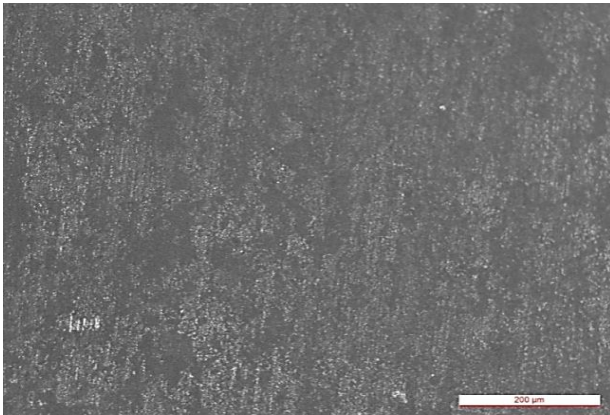


Figure 4: Graphical analysis of experimental and model value with a set of reaction

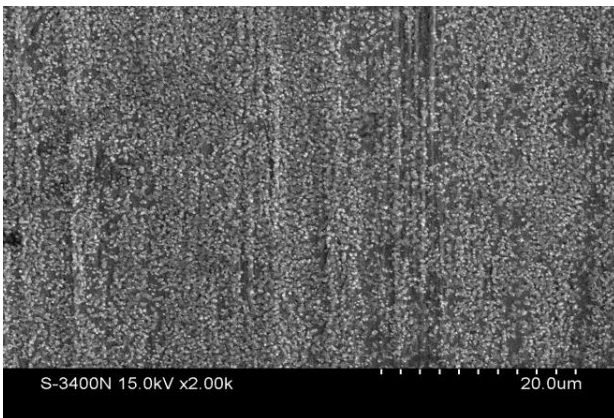
lar rolled structures are quite clearly observed in both Figures 5a and 5b. The orientation of the grains is longitudinal as observed through optical microscope but the directional validation is specified by Scanning Electron Microscope. A clear contrast is observed between the etched and non-etched specimens. The mechanically processed sample is quite prominent.

3.4.2 Optical microscopy and scanning electron microscopy of the as-deposited optimized sample

Figure 6a shows the optical microstructure of electroless deposits over the copper substrate. Round shaped particles of varying sizes are observed under the optical microscope. Although some of the structures are larger than



(a) Optical Microscopy Image of copper substrate with ferric chloride (FeCl_2) etching



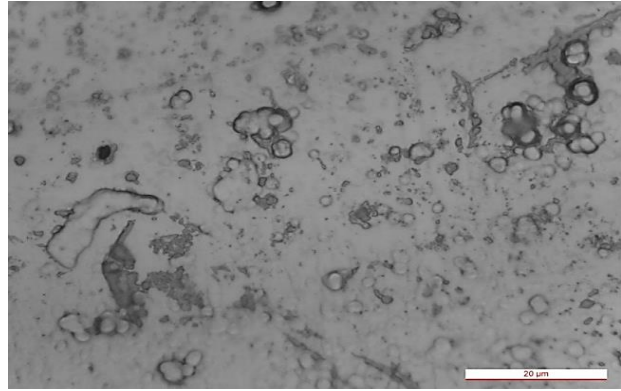
(b) SEM image of the copper substrate without etching

Figure 5

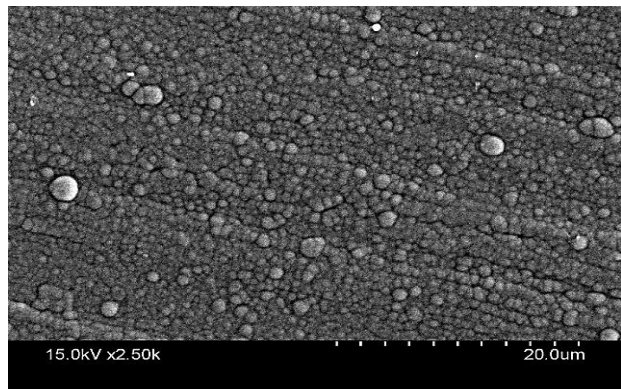
the rest, clustering of particles is also observed. Figure 6b shows the SEM microphotograph of optimized Ni-Co-P coating. Spherical grains are dispersed over the entire surface. Surface structures showed no cracks on the entire surface. A dense and compact Ni-Co-P coating is visible over the substrate by the phosphides prepared by the electroless chemical bath. It contributes to the reduction of porosity of the deposited layer further by enhancing the surface roughness of the electroless Ni-Co-P coating. A strong conglomeration of particles of fine deposition has been found on the surface structure of varying spherical particles.

3.4.3 EDX analysis of the optimized coating

EDX was done in the AZTEC software using the OXFORD X-max50 machine to find the weight percentage of different elements. The corresponding EDX analysis is shown in Fig-



(a) Optical Microscopy film of Optimized sample with dilute HCl and FeCl_2 etching



(b) Scanning Electron Microscopy micrograph of the optimized coating

Figure 6

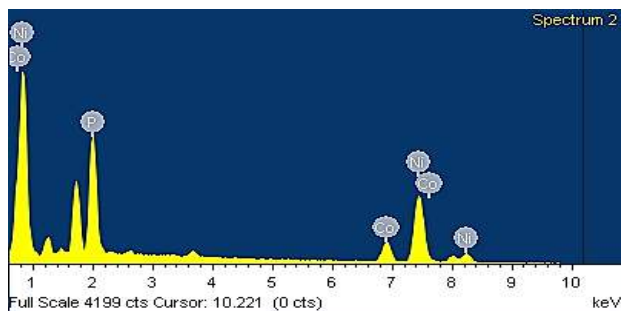
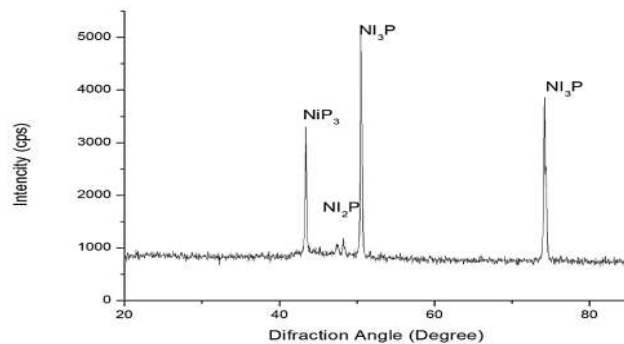


Figure 7: EDX analysis of the optimized coating

ure 7 which depicts the presence of elemental Ni, Co, and P in the optimize coated substrate. Table 6 illustrates the elemental weight percentage in the substrate after melting. This study reveals that this is a high-phosphorous content coating [4]. Excellent anti-corrosion and minimum surface roughness properties are observed in the case of high-phosphorous content coating which was depicted in a study by M. Czagány *et al.* [34].

Table 6: Elemental weight percentage of the coating

Element	Weight percentage (%)
Nickel	66.58
Cobalt	15.68
Phosphorus	17.74
Total	100.00

**Figure 8:** XRD plot of the optimized coated sample

3.4.4 XRD analysis of the optimized coated sample

X-ray diffraction analysis of the optimized coating is done by X-ray diffraction in RigakuUltima-III machine, using Cu $K\alpha$ radiation in the range of 2θ from 20° to 80° with a scan speed of 5° min^{-1} and the presence of varying size of the phases are visualized. Figure 8 demonstrates the XRD analysis of the optimum substrate structures of the as-deposited Ni-Co-P coating. The presence of Ni_2P , NiP_3 , Ni_3P phases in the coating is observed from Figure 8. The presence of these phases completely depends upon the concentration of cobalt sulfate, sodium hypophosphite, and bath temperature. It is due to the presence of Ni_3P phases that the surface roughness of the coated sample is lower than usual [35, 36].

4 Conclusion

From the performed experiment and the optimization process, it has been revealed that 15 g/L of cobalt sulphate, 25 g/L of sodium hypophosphite and 85°C were the optimized conditions to obtain a surface roughness of $0.913\mu\text{m}$. The surface roughness of the copper substrate was originally $1.19\mu\text{m}$. Clearly, one can conclude that the optimized as-deposited coated substrate shows a significant decrease of 23.3% in surface roughness as compared to the original copper substrate. The optimized model values and the experimental values are identical, thus proving this model to

be a savior of cost and time simultaneously. Hence, there will be no such need to perform experiments in the industries in order to predict the surface roughness of the coating since it can be predicted through this technique itself. ANOVA results showed that cobalt sulphate along with all the three interactions were significant in determining the surface roughness of the coating. SEM results have revealed granular grain structures of the coating while XRD analysis showed the presence of three phases (Ni_2P , NiP_3 , Ni_3P) in the coated substrate. EDX analysis showed the weight percentages of nickel, cobalt, and phosphorus in the optimized coating.

Acknowledgement: The authors would like to thank Professor Deb Dulal Das of IEST Shibpur for the SEM and EDX analysis.

References

- [1] Brenner A., Riddell G., Deposition of nickel and cobalt by chemical reduction, *J. Res. Natl. Bur. Stand.*, 1947, 39(5), 385.
- [2] Agarwala R.C., Agarwala V., Electroless alloy/composite coatings: A review, *Sadhana*, 2003, 28(3-4), 475-493.
- [3] Wang S.-C., Wei W.-C.J., Kinetics of electroplating process of nano-sized ceramic particle/Ni composite, *Mater. Chem. Phys.*, 2003, 78(3), 574-580.
- [4] Sudagar J., Lian J., Sha W., Electroless nickel, alloy, composite and nano coatings - A critical review, *J. Alloys Compd.*, 2013, 571, 183-204.
- [5] Oraon B., Majumdar G., Ghosh B., Improving hardness of electroless Ni-B coatings using optimized deposition conditions and annealing, *Mater. Des.*, 2008, 29(7), 1412-1418.
- [6] Liu Y., Zhao Q., Study of electroless Ni-Cu-P coatings and their anti-corrosion properties, *Appl. Surf. Sci.*, 2004, 228(1-4), 57-62.
- [7] Alirezai S., Monirvaghefi S.M., Salehi M., Saatchi A., Wear behavior of Ni-P and Ni-P-Al 2O_3 electroless coatings, *Wear*, 2007, 262(7-8), 978-985.
- [8] Ebrahimian-Hosseiniabadi M., Azari-Dorcheh K., Moonir Vaghefi S.M., Wear behavior of electroless Ni-P-B4C composite coatings, *Wear*, 2006, 260(1-2), 123-127.
- [9] Nascimento M., Effects of surface treatments on the fatigue strength of AISI 4340 aeronautical steel, *Int. J. Fatigue*, 2001, 23(7), 607-618.
- [10] Xu Y., Jiang F., Newbern S., Huang A., Ho C.-M., Tai Y.-C., Flexible shear-stress sensor skin and its application to unmanned aerial vehicles, *Sens. Actuators Phys.*, 2003, 105(3), 321-329.
- [11] Trudgeon M.A., Griffiths J.R., Corrosion resistance of electroless nickel coatings in mining environments, *Br. Corros. J.*, 1986, 21(2), 113-118.
- [12] Katz A., Redlich M., Rapoport L., Wagner H.D., Tenne R., Self-lubricating coatings containing fullerene-like WS 2 nanoparticles for orthodontic wires and other possible medical applications, *Tribol. Lett.*, 2006, 21(2), 135-139.
- [13] Yasutake Y., Kono K., Kanehara M., Teranishi T., Buitelaar M.R., Smith C.G. et al., Simultaneous fabrication of nanogap gold elec-

- trodes by electroless gold plating using a common medical liquid, *Appl. Phys. Lett.*, 2007, 12, 91(20), 203107.
- [14] Zhao H.-B., Pflanz K., Gu J.-H., Li A.-W., Stroh N., Brunner H. et al., Preparation of palladium composite membranes by modified electroless plating procedure, *J. Membr. Sci.*, 1998, 142(2), 147-157.
- [15] Balaraju J.N., Raman N., Manikandanath N.T., Nanocrystalline electroless nickel poly-alloy deposition: incorporation of W and Mo, *Trans. IMF*, 2014, 92(3), 169-176.
- [16] Krishnan K.H., John S., Srinivasan K.N., Praveen J., Ganesan M., Kavimani P.M., An overall aspect of electroless Ni-P depositions - A review article, *Metall. Mater. Trans. A*, 2006, 37(6), 1917-1926.
- [17] Krishnaveni K., Sankara Narayanan T.S.N., Seshadri S.K., Electroless Ni-B coatings: preparation and evaluation of hardness and wear resistance, *Surf. Coat. Technol.*, 2005, 190(1), 115-21.
- [18] Brown R.J.C., Brewer P.J., Milton M.J.T., The physical and chemical properties of electroless nickel-phosphorus alloys and low reflectance nickel-phosphorus black surfaces, *J. Mater. Chem.*, 2002, 12(9), 2749-2754.
- [19] Cui G., Li N., Li D., Zheng J., Wu Q., The physical and electrochemical properties of electroless deposited nickel-phosphorus black coatings, *Surf. Coat. Technol.*, 2006, 200(24), 6808-6814.
- [20] Sahoo P., Das S.K., Tribology of electroless nickel coatings - A review, *Mater. Des.*, 2011, 32(4), 1760-1775.
- [21] Bucher J.P., Douglass D.C., Bloomfield L.A., Magnetic properties of free cobalt clusters, *Phys. Rev. Lett.*, 1991, 66(23), 3052-3055.
- [22] Halbach K., Physical and optical properties of rare earth cobalt magnets, *Nucl. Instrum. Methods Phys. Res.*, 1981, 187(1), 109-117.
- [23] Li Y., Wang R., Qi F., Wang C., Preparation, characterization and microwave absorption properties of electroless Ni-Co-P-coated SiC powder, *Appl. Surf. Sci.*, 2008, 254(15), 4708-4715.
- [24] Rapp R.A., Maak F., Thermodynamic properties of solid copper-nickel alloys, *Acta Metall.*, 1962, 10(1), 63-69.
- [25] Gao Y., Huang L., Zheng Z.J., Li H., Zhu M., The influence of cobalt on the corrosion resistance and electromagnetic shielding of electroless Ni-Co-P deposits on Al substrate, *Appl. Surf. Sci.*, 2007, 253(24), 9470-9475.
- [26] Mejias A., Chicot D., Pertuz A., Iost A., Montagne A., Cadenas P., Hardness evaluation from a bilayer coating system of Ni-P deposited on carbon steel plates by multicycle indentation tests, *Surf. Coat. Technol.*, 2018, 334, 410-419.
- [27] Hou C.-C., Li Q., Wang C.-J., Peng C.-Y., Chen Q.-Q., Ye H.-F. et al., Ternary Ni-Co-P nanoparticles as noble-metal-free catalysts to boost the hydrolytic dehydrogenation of ammonia-borane, *Energy Environ. Sci.*, 2017, 10(8), 1770-1776.
- [28] Sankara Narayanan T.S.N., Selvakumar S., Stephen A., Electroless Ni-Co-P ternary alloy deposits: preparation and characteristics, *Surf. Coat. Technol.*, 2003, 172(2-3), 298-307.
- [29] Loto C.A., Electroless Nickel Plating - A Review, *Silicon*, 2016, 8(2), 177-186.
- [30] Majumdar G., Biswas N., Pramanik A., Sen R.S., Chakraborty M., Optimization of mass deposition and surface roughness for ternary Ni-Cu-P electroless coating using VIKOR method, *Adv. Mater. Process. Technol.*, 2017, 3, 3(2), 186-195.
- [31] Mukhopadhyay A., Duari S., Barman T.K., Sahoo P., Optimization of Friction and Wear Properties of Electroless Ni-P Coatings Under Lubrication Using Grey Fuzzy Logic, *J. Inst. Eng. India. Ser. D*, 2017, 98(2), 255-268.
- [32] Palaniappa M., Seshadri S.K., Friction and wear behavior of electroless Ni-P and Ni-W-P alloy coatings, *Wear*, 2008, 265(5-6), 735-740.
- [33] Sarkar S., Baranwal R.K., Biswas C., Majumdar G., Haider J., Optimization of process parameters for electroless Ni-Co-P coating deposition to maximize micro-hardness, *Mater. Res. Express*, 2019, 18, 6(4), 046415.
- [34] Czagány M., Baumli P., Kaptay G., The influence of the phosphorous content and heat treatment on the nano-micro-structure, thickness and micro-hardness of electroless Ni-P coatings on steel, *Appl. Surf. Sci.*, 2017, 423, 160-169.
- [35] Lin J.-D., Chou C.-T., The influence of phosphorus content on the microstructure and specific capacitance of etched electroless Ni-P coatings, *Surf. Coat. Technol.*, 2019, 368, 126-137.
- [36] Hadipour A., Rahsepar M., Hayatdavoudi H., Fabrication and characterisation of functionally graded Ni-P coatings with improved wear and corrosion resistance, *Surf. Eng.*, 2019, 35(10), 883-890.